



# Modular access to alkylgermanes via reductive germulative alkylation of activated olefins under nickel catalysis

Received: 19 April 2023

Accepted: 13 November 2023

Published online: 23 November 2023

Check for updates

Rui Gu<sup>1,2</sup>, Xiujuan Feng<sup>2</sup>, Ming Bao<sup>2</sup>✉ & Xuan Zhang<sup>1,2</sup>✉

Carbon-introducing difunctionalization of C-C double bonds enabled by transition-metal catalysis is one of most straightforward and efficient strategies to construct C-C and C-X bonds concurrently from readily available feedstocks towards structurally diverse molecules in one step; however, analogous difunctionalization for introducing germanium group and other functionalities remains elusive. Herein, we describe a nickel-catalyzed germulative alkylation of activated olefins with easily accessible primary, secondary and tertiary alkyl bromides and chlorogermanes as the electrophiles to form C-Ge and C-C<sub>alkyl</sub> bonds simultaneously. This method provides a modular and facile approach for the synthesis of a broad range of alkylgermanes with good functional group compatibility, and can be further applied to the late-stage modification of natural products and pharmaceuticals, as well as ligation of drug fragments. More importantly, this platform enables the expedient synthesis of germanium substituted ospemifene-Ge-OH, which shows improved properties compared to ospemifene in the treatment of breast cancer cells, demonstrating high potential of our protocol in drug development.

Due to their abundance and widespread availability of alkenes, difunctionalization processes that introduce two functional groups on each side of C-C double bonds<sup>1-12</sup> has emerged as a versatile and powerful tool for rapid construction of high-value and complex molecular scaffolds in a single operation. Over the past decade, transition-metal catalysis<sup>13-20</sup> has drawn great attention, because it enables these reactions to proceed with good selectivity and high efficiency. Among them, carbonized difunctionalization of olefins<sup>21-26</sup> is well developed (Fig. 1a, path a), which provides attractive manipulations for creation of C-C and C-X bonds simultaneously. Despite such impressive advances, employing carbon group elements in difunctionalization of alkenes under transition-metal catalysis, such as germanium<sup>27-29</sup> for preparing organogermanes (Fig. 1a, path b), remains underdeveloped.

Germanium is in the same column of periodic table as carbon atom, but possesses different electronegativity and atom radius. Therefore, Germanium is generally considered as a bioisostere of carbon in medical chemistry<sup>30,31</sup> for biological and pharmacological studies, because of their relatively high robustness, hydrophobicity and low toxicity. In addition, organogermanes have also been applied to functional material areas<sup>32-34</sup>, such as molecular electronics, nanoscale lithography, and biosensors. Aside from above applications, organogermanium compounds have led to increased interest in the investigation of their reactivities in organic synthesis and catalysis<sup>35-42</sup>. As such, synthetic access to germanium-containing architectures by a general and effective way is highly appealing, but challenging. Traditionally, construction of these molecules predominantly relies on organometallic reactivity through the nucleophilic substitution of a

<sup>1</sup>School of Chemistry and Materials Science, Institute of Advanced Materials and Flexible Electronics (IAMFE), Nanjing University of Information Science and Technology, 219 Ningliu Road, Nanjing 210044, China. <sup>2</sup>State Key Laboratory of Fine Chemicals, School of Chemical Engineering, Dalian University of Technology, 2 Linggong Road, Dalian 116024, China. ✉e-mail: [mingbao@dlut.edu.cn](mailto:mingbao@dlut.edu.cn); [xuanzhang@nuist.edu.cn](mailto:xuanzhang@nuist.edu.cn)

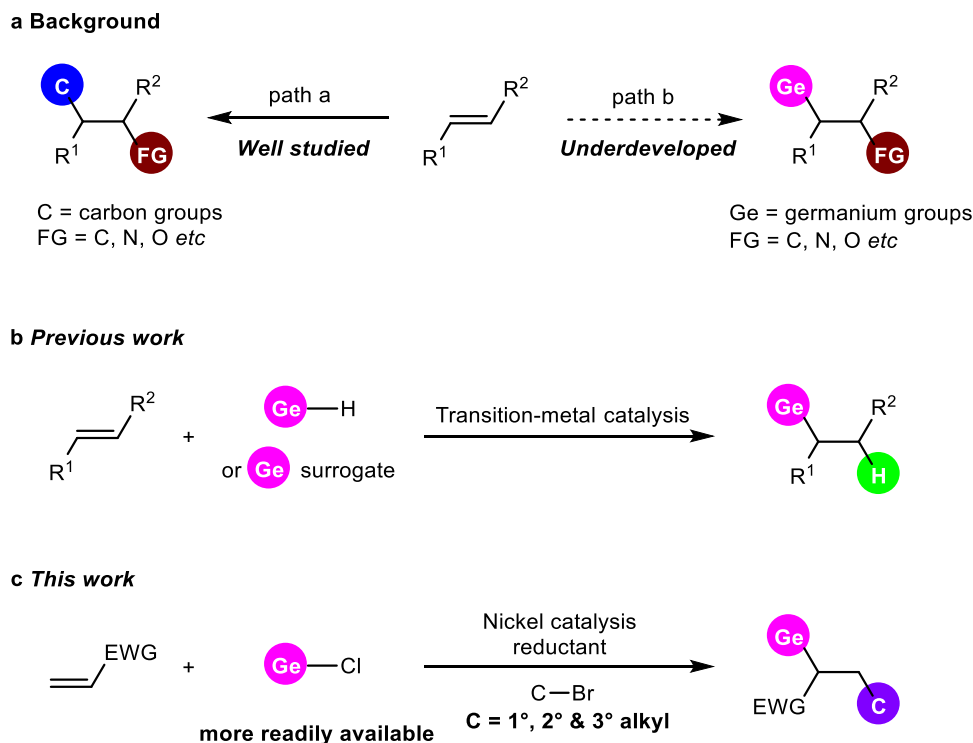


**Fig. 1 | Difunctionalization of alkenes and germlyative functionalization of alkenes.** **a** difunctionalization of alkenes. **b** germlyative hydrogenation of alkenes. **c** reductive germlyative alkylation of alkenes. EWG electron-withdrawing groups.

The carbon groups are colored in blue. The common functional groups are colored in brown. The germanium groups are colored in pink. The hydrogen atom is colored in green. The alkyl groups are colored in purple.

germyl electrophile by Grignard<sup>43</sup> or organolithium<sup>44</sup> reagents or, vice versa, by a nucleophilic germanium reagent<sup>45–47</sup> reacting with electrophiles. However, the need of pre-generation and difficulty in handling of organometallic reagents, and their high reactivity without discrimination undoubtedly limit the functional group compatibility. Catalytic approaches for synthesizing organogermanes including cross-coupling reactions<sup>48–52</sup>, C–H bond germylations<sup>53–56</sup> have not been achieved until recently, where palladium, rhodium or nickel catalysis were employed. These processes typically use  $\text{Me}_3\text{Ge-GeMe}_3$ ,  $\text{R}_3\text{GeH}$ , or  $\text{R}_3\text{Ge-Zn}$  as the germyl reagents. Despite such formidable progresses, their synthetic applications are still restricted by several critical disadvantages such as multiple-step synthesis, limited substrate scope and hardly available germyl sources. Hence, given the importance of expanding the chemical space of alkene difunctionalization and providing a synthetic toolbox to create germanium-substituted molecules with diverse and complex structures for exploring their application potential, developing a new strategy through germlyative transformation of olefins to install germyl groups into organic motifs with easily accessible substrates and convenient germyl sources would be greatly attractive and beneficial.

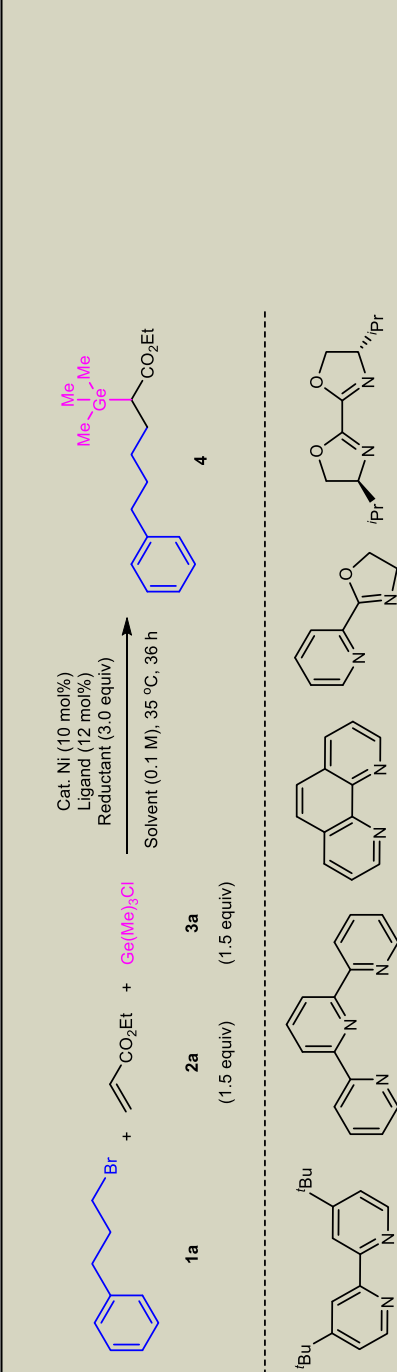
Works to construct C–Ge bonds via alkene difunctionalization have emerged over past years<sup>27–29,57–65</sup>. But it's worth noting that transition-metal catalyzed hydrogermylations are most frequently studied<sup>57–62</sup>, which introduce a germyl group on one side of C–C double bond and only a hydrogen atom on the other position (Fig. 1b). These monofunctionalized protocols largely reduce the complexity and diversity of germanium-containing molecules, and consequently diminish their further application. In contrast, germlyative alkylation of alkenes enabled by transition-metal catalysis would be much more fascinating but still unexplored. The introduction of alkyl groups can not only significantly increase structural complexity of molecules, but also work as useful descriptors for greater three-dimensional shape compared to flat arenes, and more likely to succeed as drug candidates because of their better match with biological targets which have 3D

structures<sup>66–68</sup>. Herein, we report a nickel catalyzed reductive germlyative alkylation of activated olefins using both readily available unactivated alkyl bromides and chlorogermanes as the starting materials (Fig. 1c). In this work, a modular and general method under mild conditions to access alkylgermanes with high molecular diversity is presented, which exhibits broad substrate scope, good functionality tolerance and high potential for improving efficacy of drug via structure modification.

## Results and discussion

### Reaction discovery

To evaluate the desired reaction, we selected (3-bromopropyl)benzene **1a** as the model alkyl source, ethyl acrylate **2a** as the alkene unit, chlorotrimethylgermane **3a** as the germanium reagent,  $\text{NiBr}_2\cdot\text{DME}$  as the precatalyst, 4,4'-di-*tert*-butyl-2,2'-bipyridine **L1** as the ligand and manganese powder as the reductant to initiate the optimization studies. The mixture was stirred in *N,N*-dimethyl acetamide (DMA) at 35 °C for 36 h under a  $\text{N}_2$  atmosphere to afford the desired product ethyl 6-phenyl-2-(trimethylgermyl)hexanoate **4** in 15% assay yield, along with 41% of recovered **1a** (Table 1, entry 1) and side products including hydro-debromination of **1a**, dehydrobromination of **1a** and hydroalkylation of **2a** (for details, see the Supplementary Table 1). Encouraged by the promising result, we further investigated a variety of ligands with different skeletons; compared with pyridine-containing ligands, the bisoxazoline ligand **L5** gave the best reactivity with good mass balance (Table 1, entries 2–5). Then, a set of nickel precatalysts were examined in the presence of **L5**, and  $\text{NiBr}_2$  was found to be optimal, which improves the yield of product **4** to 73% (Table 1, entries 6–9). Surprisingly, the reaction proceeds better in the absence of ligand **L5** using  $\text{NiBr}_2$  as the catalyst to give a yield up to 86% yield (Table 1, entry 10). Subsequently, solvent effects were studied under the ligand-free conditions, and the observations indicate the solvent has a big impact on the reaction performance. Among the solvents studied, DMA represents the best choice, and other solvents, such as

**Table 1 | Optimization of reaction conditions<sup>a</sup>**


Entry	Cat. Ni	Ligand	Reductant	Solvent	Yield of <b>4</b> (%)	Recovery of <b>1a</b> (%)
1	NiBr <sub>2</sub> ·DME	L1	Mh	DMA	15	41
2	NiBr <sub>2</sub> ·DME	L2	Mh	DMA	4	1
3	NiBr <sub>2</sub> ·DME	L3	Mh	DMA	19	57
4	NiBr <sub>2</sub> ·DME	L4	Mh	DMA	3	62
5	NiBr <sub>2</sub> ·DME	L5	Mh	DMA	35	50
6	NiBr <sub>2</sub>	L5	Mh	DMA	73	7
7	Ni(acac) <sub>2</sub>	L5	Mh	DMA	30	50
8	Ni(PPh <sub>3</sub> ) <sub>2</sub> Cl <sub>2</sub>	L5	Mh	DMA	5	87
9	Ni(COD) <sub>2</sub>	L5	Mh	DMA	37	49
10	NiBr <sub>2</sub>	—	Mh	DMA	86 (80 <sup>b</sup> )	2
11	NiBr <sub>2</sub>	—	Mh	DMSO	trace	37
12	NiBr <sub>2</sub>	—	Mh	CH <sub>3</sub> CN	4	91
13	NiBr <sub>2</sub>	—	Mh	EtOAc	0	100
14	NiBr <sub>2</sub>	—	Zn	DMA	6	88
15	NiBr <sub>2</sub>	—	TDAE	DMA	1	43
16 <sup>c</sup>	NiBr <sub>2</sub>	—	Mh	DMA	53	25
17 <sup>d</sup>	NiBr <sub>2</sub>	—	Mh	DMA	71	1
18 <sup>e</sup>	NiBr <sub>2</sub>	—	Mh	DMA	77	1

<sup>a</sup>Reaction conditions: **1a** (0.1 mmol), **2a** (0.15 mmol), **3a** (0.15 mmol), Ni catalyst (10 mol%), ligand (12 mol%), reductant (12 mol%), solvent (1 mL), 35 °C, 36 h, N<sub>2</sub> atmosphere. Yields are determined by GC using dodecane as the internal standard.

<sup>b</sup>The isolated yield was shown in parentheses on 0.3 mmol scale.

<sup>c</sup>NiBr<sub>2</sub> (5 mol%) was used.

<sup>d</sup>**2a** (0.12 mmol) was used.

<sup>e</sup>**3a** (0.12 mmol) was used. DME dimethyl ether, DMA *N,N*-dimethylacetamide, acac acetylacetonate, COD 1,5-cyclooctadiene, COD 1,5-cyclooctadiene, DMSO dimethyl sulfoxide, EtOAc ethyl acetate, TDAE tetraakis(dimethylamino)ethylene.

dimethyl sulfoxide (DMSO), acetonitrile, ethyl acetate (EtOAc) almost suppress the reaction (Table 1, entries 11-13). After that, several reductants were screened; zinc powder and tetrakis(dimethylamino) ethylene (TDAE) show much lower reactivity, and manganese remains the suitable reagent (Table 1, entries 14 and 15). Reducing the catalytic loading of NiBr<sub>2</sub> resulted in decreased yield of 53% (Table 1, entry 16). The utilization of less amount of alkene **2a** or chlorogermane **3a** also lowered the reaction efficiency (Table 1, entries 17 and 18). Ultimately, the optimized conditions were identified as follows: NiBr<sub>2</sub> (10 mol%) and Mn (3 equiv.) in DMA (0.1 M) at 35 °C for 36 h (Table 1, entry 10).

### Substrate scope

With the optimized set of reaction conditions in hand, the scope of this new transformation was then investigated (Fig. 2). Choosing ethyl acrylate **2a** and chlorotrimethylgermane **3a** as the representative substrates, the generality of unactivated alkyl halides was explored first. Besides (3-bromopropyl)benzene **1a**, (3-iodopropyl)benzene **1a'** and (3-chloropropyl)benzene **1a''** were also investigated under standard conditions, in which different reactivities were obtained for synthesis of product **4** (52% yield from **1a'** and no product from **1a''**).

Various (2-bromoethyl)benzene derivatives **1b-1g** including electron-donating groups (-OMe and -NH<sub>2</sub>) and electron-withdrawing groups (-Cl, -Br, -CO<sub>2</sub>Me and -CF<sub>3</sub>) substituted on the phenyl ring were compatible, which smoothly underwent germylalkylation reactions to produce desired products **5-10** in good yields (58%-80%). Given the prevalence of heteroaryl rings in drug molecules, we were delighted to find that a number of heterocycle-containing alkyl bromides could also be successfully coupled in this reaction. A range of five- and six-membered heteroarenes, such as thiophene, benzofuran, indole, carbazole and quinoline all survived well in the reductive conditions (**11-15**). Notably, substrate with coordinating Lewis basic N(sp<sup>2</sup>) atom (**15**) can work with slightly modified conditions. All-carbon alkyl bromides, 1-bromobutane **1m** and (bromomethyl)cyclobutene **1n** are undoubtedly suitable substrates under the three-component reaction conditions to afford corresponding alkylgermanes **16** and **17** in good yields (64% and 72%). The conditions were also applicable to a plenty of valuable functionalized units (**18-31**) including some potentially sensitive functional groups and useful synthetic handles, such as ketone (**22**), acetal (**27**), tertiary amine (**30**), chloride (**20**), nitrile (**23**), alkenes (**25** and **26**), phosphate (**28**), sulfone (**29**) and boronic ester (**31**), which

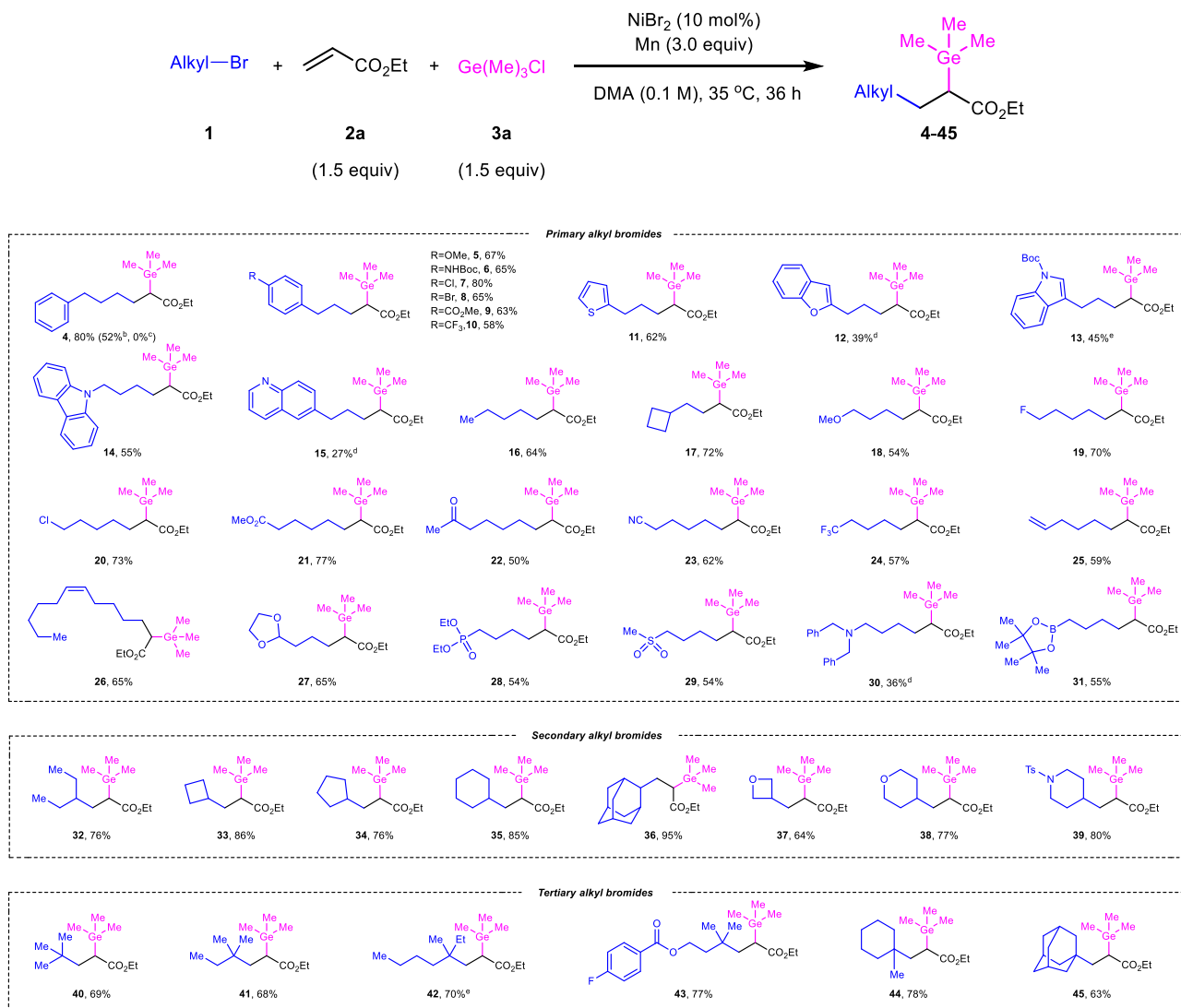


**Fig. 2 | The scope of alkyl bromides.** <sup>a</sup>Reaction conditions: **1** (0.3 mmol), **2a** (0.45 mmol), **3a** (0.45 mmol), NiBr<sub>2</sub> (10 mol%), Mn (0.9 mmol), DMA (3 mL), 35 °C, 36 h, N<sub>2</sub> atmosphere. Isolated yield was shown. <sup>b</sup>(3-iodopropyl)benzene was used instead of (3-bromopropyl)benzene. <sup>c</sup>(3-chloropropyl)benzene was used instead of

(3-bromopropyl)benzene. <sup>d</sup>**L5** (12 mol%) was used as the additive. <sup>e</sup>diastereomeric ratio can't be determined by Proton Nuclear Magnetic Resonance and High Performance Liquid Chromatography. Boc tert-butyloxycarbonyl, Ts tosyl.

can provide a good chance to produce more structurally diverse organogermanes after corresponding modifications. Notably, reactive functional groups such as boronic esters, which is commonly problematic in transition-metal-catalyzed reactions, could also be tolerated well in this reaction (**31**). Then, we turn to explore secondary and tertiary alkyl bromides. The reaction of 3-bromopentane **1a** with alkene **2a** and chlorogermane **3a** proceeded smoothly under standard conditions to deliver desired germylated alkyl carboxylic ester **32** in 76% yield. Cycloalkyl groups with ring sizes ranging from four to six and 2-adamantyl were all amenable in our system to give carbocycle derivatives **33–36** in good yields (76%–95%). Moreover, alkyl bromides **1ak–1am** bearing various saturated heterocycles were studied, which were demonstrated to be suitable substrates with good efficiency (**37–39**, 64%–80%). Meanwhile, acyclic and cyclic tertiary carbons on alkyl bromides were successfully tolerated in this protocol to construct quaternary carbon center-containing alkyl germanium compounds **40–45** in decent yields (63–78%). Groups such as hydroxyls, aldehydes, alkynes and amides were not amenable in current system, which gave the target products in <10% yields (for details, see the Supplementary Information).

Next, we focused on evaluating the scope of activated olefins and chlorogermanes utilizing (3-bromopropyl)benzene **1a** as the alkylating reagent (Fig. 3). A set of acrylates **2b–2d** underwent the target transformation smoothly, providing the products **46–48** in 61%–76% yields. Other types of activated alkenes like acrylamide **2e**, acrylonitrile **2f**, (vinylsulfonyl)benzene **2g** and diethyl vinylphosphonate **2h** were also amenable to the reaction with reasonable efficiency under slightly modified conditions (**49–52**, 34%–68%). In addition, steric hindered methyl methacrylate **2i** and dimethyl itaconate **2j** could be transformed into quaternary carbon centers substituted with a germyl group in synthetically useful yields (**53** and **54**). Unfortunately,  $\beta$ -substituted acrylates including methyl (*E*)-but-2-enoate, 5,6-dihydro-2H-pyran-2-one and methyl cyclopent-1-ene-1-carboxylate as well as styrene were all incompatible substrates (for details, see the Supplementary Information). Following, the reactivity of chlorogermanes were examined by varying substituents on germanium atom. As expected, the reactions of chlorotrialkylgermanes **3b–3d** possessing longer alkyl chain can proceed with similar efficiency compared to the standard reaction employing chlorotrimethylgermane **3a** (**55–57**). The arylated germanium-containing products **59–60** were observed in good to high yields with phenyl substituted chlorogermanes **3e–3g** as the starting materials under optimal conditions. These results indicate there is no obvious substituent effect on germanium reagent.

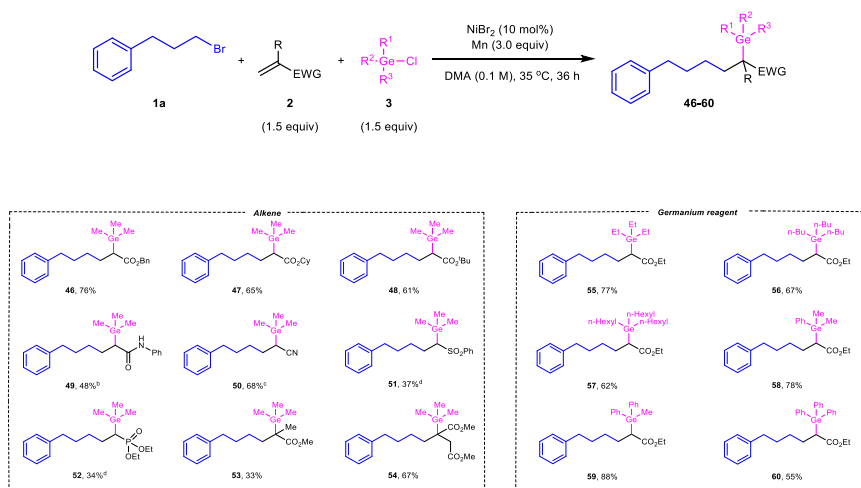


**Fig. 3 | The scope of alkenes and germanium reagents<sup>a</sup>.** <sup>a</sup>Reaction conditions: **1a** (0.3 mmol), **2** (0.45 mmol), **3** (0.45 mmol), NiBr<sub>2</sub> (10 mol%), Mn (0.9 mmol), DMA (3 mL), 35 °C, 36 h, N<sub>2</sub> atmosphere. Isolated yield was shown. <sup>b</sup>L5 (12 mol%) was

Taking account of the broad substrate scope and good functional group compatibility of this protocol, we were encouraged to use the developed reaction for modifying drug molecules (Fig. 4). Alkyl bromides derived from commercial drugs, such as ospemifene, probenecid, (1*R*)-(+)-Camphanic acid, oxaprozin and triclosan were all straightforwardly modified through the three-component reaction with alkene **2a** and chlorogermane **3a**, which opens a new direction for downstream derivatizations (**61–65**). On the other hand, pharmaceutically relevant olefins were also subjected to the reaction conditions. For example, olefins bearing L-menthol (**66**) and indomethacin (**67**) were coupled in 66% and 46% yields, respectively. Lastly, complex molecule **68** having two pharmacophores (L-menthol and probenecid) was easily obtained with this transformation, demonstrating the applicable potential of our protocol in drug discovery.

### Synthetic applications

The practicality of the germylative alkylation reaction was showcased by gram-scale reaction of model substrates, delivering target product **4** in 1.33 g with similar efficiency (79% versus 80%). The  $\beta$ -hydroxy alkylgermane **69** was directly synthesized from the reduction of **4** in the presence of LiAlH<sub>4</sub> (Fig. 5a). Moreover, the alkylgermane **4** can be converted into  $\beta$ -hydroxy carboxylate **70** in the presence of TBAF via degermylative addition with benzaldehyde (Fig. 5a), which is a valuable building blocks. Ethyl 2,6-dibromo-6-phenylhexanoate **71**, bearing similar structure with a classical synthon- $\alpha$ -bromo carboxylate, was accessed through the degermylative dibromination of **4** (Fig. 5a). Ospemifene (Ospemifene), approved by the U.S. Food and Drug Administration, is used for the treatment of moderate to severe dyspareunia (vaginal and vulvar atrophy associated with menopause). It has shown the bioactivity in the prevention of breast cancer<sup>69,70</sup> as a novel Selective Estrogen Receptor Modulator (SERM) that acts as an agonist in brain, bone and vagina and acts as an antagonist in uterus and breasts, which possesses ideal characteristics of a SERM. Although this drug has exhibited a promising pharmacological profile, the high value of half-maximal inhibitory concentration (IC<sub>50</sub>) limits its application and encourages us to modify the structure of ospemifene to pursue better efficacy. To demonstrate the potential of prepared alkylgermanes and the applicability of our method to drug discovery settings, we subsequently applied our new germylative alkylation reaction to the synthesis of germanium-containing ospemifene analog (Fig. 5b). Toward this end, ospemifene-Ge-OH **72** was afforded by **1bq** coupling with **2a** and **3a**, and followed by reduction (two steps, 35% overall yield). The synthesized ospemifene analog **72** was evaluated for its

used as the additive. <sup>c</sup>NiBr<sub>2</sub> (15 mol%), **L5** (20 mol%) was used at 50 °C, 60 h. <sup>d</sup>NiBr<sub>2</sub> (15 mol%) was used. EWG electron-withdrawing group, Bn benzyl, Cy cyclohexyl, <sup>t</sup>Bu *tert*-butyl.

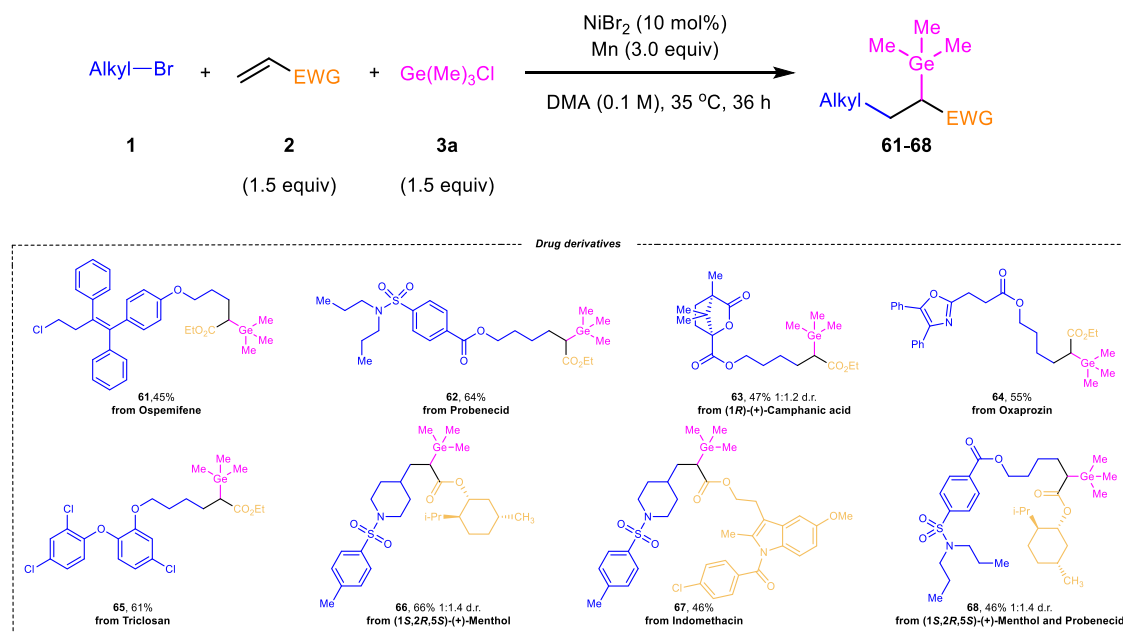


**Fig. 4 | The late-stage functionalization.** <sup>a</sup>Reaction conditions: **1** (0.2 mmol), **2** (0.3 mmol), **3a** (0.3 mmol), NiBr<sub>2</sub> (10 mol%), Mn (0.6 mmol), DMA (2 mL), 35 °C, 36 h, N<sub>2</sub> atmosphere. Isolated yield was shown. EWG electron-withdrawing group, *i*-Pr *iso*-propyl.

anti-proliferative activities against MCF-7 (ER+) and MDA-MB-231 (ER-) human breast cancer cell-lines using MTT assay (Fig. 5c, d). The IC<sub>50</sub> values showed that compound **72** was more effective against MCF-7 and MDA-MB-231 cells compared to ospemifene (45.6 μM versus 77.2 μM in MCF-7 cells, 59.58 μM versus 115.96 μM in MDA-MB-231 cells). As control, the IC<sub>50</sub> value of degermylate ospemifene-OH **73** were also measured, which were 94.09 μM for MCF-7 and 98.70 μM for MDA-MB-231 cells independently. All collected results clearly indicated that the improved anti-cancer activity is resulted from the installation of germanium group. In addition, the metabolic stability of **72** and ospemifene were explored by mouse liver microsomal metabolic assay (Fig. 5e). After 45 min of incubation in mouse microsomes, the amount of remaining **72** was higher than that of ospemifene. The calculated half-life of **72** (t<sub>1/2</sub> = 13.90 min) was ~3.6 times than that of ospemifene (t<sub>1/2</sub> = 3.82 min), suggesting the metabolic stability of ospemifene in mouse microsomes was enhanced after modification. To evaluate and compare the toxicity against normal cell between ospemifene and compound **72**, MCF-10A was chosen as the normal human cell line for studying. As shown in Fig. 5f, the semi-lethal doses of ospemifene and compound **72** against MCF-10A cell line were 53.25 μM and 158.36 μM respectively, which implied the germanium-modified molecule **72** has less toxic side effects. Lastly, we carried out a hemolysis experiment against red blood cells to access the hemocompatibility (see the Supplementary Notes and Fig. S1). Negligible hemolytic activities were observed at 120 mM for ospemifene and **72** (both of hemolysis percentage are <8%), indicating the installation of germanium group has no impact on the blood compatibility. Altogether, these results demonstrate the high potential of this germanium-introducing strategy for improving the pharmacological properties of drug candidates.

### Mechanism studies

To shed light on the possible mechanism of this reductive germylative alkylation reaction, a set of control experiments were conducted (Fig. 6). No desired product **4** was observed under model reaction conditions by adding stoichiometric amount of a radical scavenger, 2,2,6,6-tetramethyl-1-piperidinoxyl (TEMPO). Instead, radical trapping product **74** was detected by high-resolution mass spectrometry (Fig. 6a). Next, two radical-clock experiments were conducted with 6-

bromohex-1-ene (**1bv**) and (bromomethyl)cyclopropane (**1bw**) as the alkyl reagents, which are well-known radical probes. Cyclization product **76** and ring-opening products **77**, **78** were isolated in 42% and combined 62% yields, respectively. Both results indicate that an alkyl radical is produced from the alkyl bromide and involved in the reaction as a key species (Fig. 6b). In the presence of 1 equiv. Ni(COD)<sub>2</sub>, the reaction of **1a**, **2a** and **3a** in DMA at 35 °C for 36 h led to no product **4**, along with 38% of **1a** consumed. In another experiment, the catalytic reaction using 10 mol% Ni(COD)<sub>2</sub> proceeded successfully to afford target product **4** in 31% yield (Fig. 6c). These observations suggest: (1) alkyl bromide should react with nickel catalyst firstly in the reaction; (2) the manganese powder not only works as a terminal reductant, but also participates in a reductive process to generate a key reactive intermediate in the catalytic cycle.

Based on the preliminary results and previous reports<sup>51,52</sup>, a radical-type mechanism is tentatively proposed in Fig. 6d. The reaction of alkyl bromide **1** with Ni (0) generated in-situ by reduction of manganese, affords Ni (I) and an alkyl radical, which is then captured by activated olefin **2** to produce a new carbon-based radical **A**. The species **A** reacts with Ni (I) to give an alkyl-Ni (II) intermediate **B**, followed by reduction by manganese for giving a reactive alkyl-Ni (I) **C**. The oxidative addition of chlorogermane **3** with species **C** may afford alkyl-Ni (III) complex **D**, which undergoes reductive elimination to deliver the desired product.

In conclusion, we have developed a catalytic reductive germylative alkylation of activated olefins enabled by nickel catalysis under mild conditions, delivering alkylgermanes with high efficiency. This method features the direct utilizing of easily accessible alkyl bromides and chlorogermanes as the reaction partners, avoiding pre-preparation of sensitive organometallics that are often tedious to handle. The developed approach can tolerate a broad range of functional groups as well as natural products and pharmaceuticals, thereby provides a powerful tool towards highly structure-diverse aliphatic germanes including previously inaccessible motifs. Furthermore, the better pharmacological properties of the germanium-modified ospemifene compound **72** against breast cancer cells were observed by a number of biological experiments, highlighting the synthetic value and power of the present protocol. Given the generality and practicality of

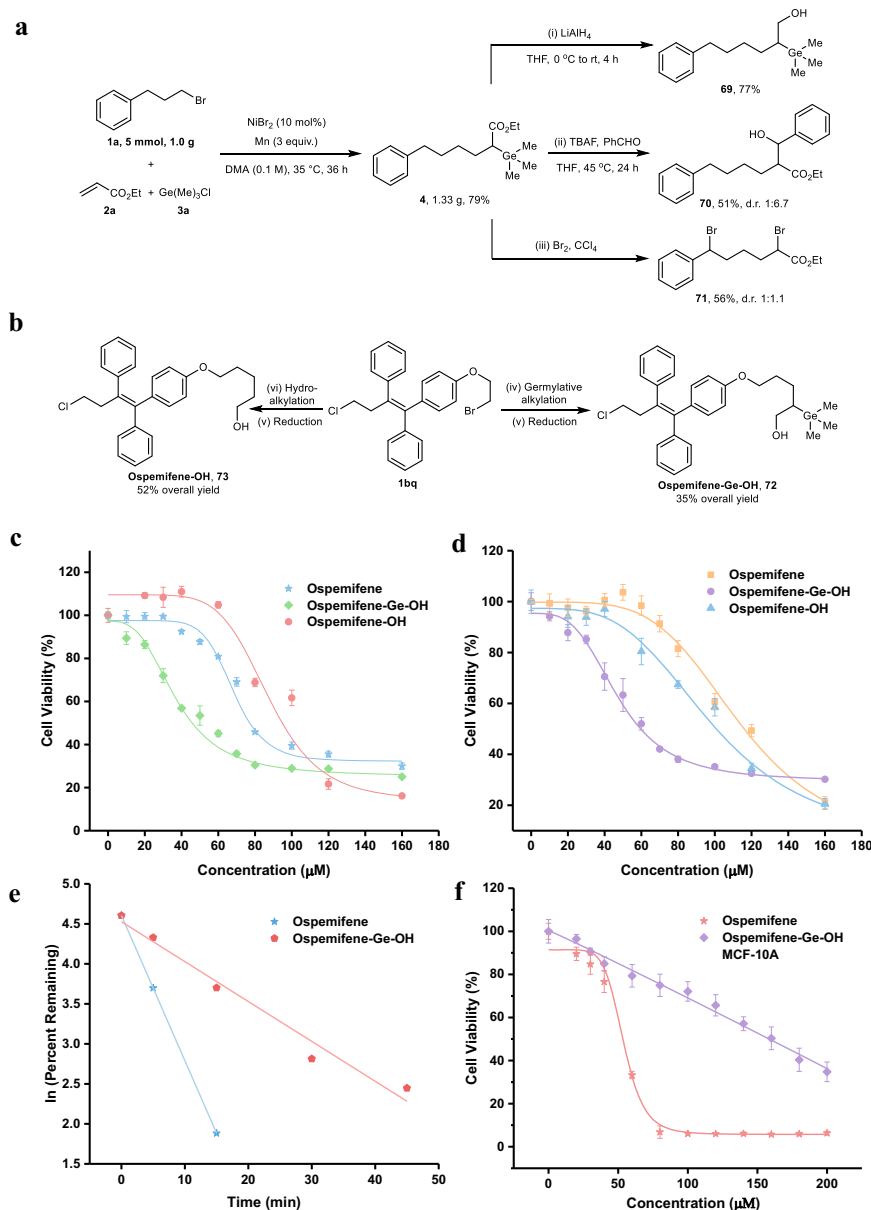


**Fig. 5 | Synthetic applications.** **a** gram-scale reaction of **1a**, **2a** and **3a**, and transformations of **4**; **4** (0.2 mmol),  $\text{LiAlH}_4$  (0.1 mmol), THF (2 mL), 0 °C, 4 h,  $\text{N}_2$  atmosphere; (ii) **4** (0.2 mmol), TBAF (0.24 mmol), PhCHO (0.24 mmol), THF (0.4 mL), 45 °C, 24 h,  $\text{N}_2$  atmosphere; (iii) **4** (0.2 mmol),  $\text{Br}_2$  (0.2 mmol),  $\text{CCl}_4$  (10 mL), 0 °C to room temperature, 3.5 h,  $\text{N}_2$  atmosphere; (b) synthetic route of compounds **72** and **73**; (iv) standard condition; (v) **61** (0.2 mmol),  $\text{LiAlH}_4$  (0.1 mmol), THF (2 mL), 0 °C, 4 h,  $\text{N}_2$  atmosphere; (vi) **1bq** (1 mmol),  $\text{NiCl}_2(\text{PPh}_3)_2$  (0.1 mmol), Zn (2.5 mmol), ethyl acrylate (4 mmol),  $\text{H}_2\text{O}$  (1 mmol),  $\text{CH}_3\text{CN}$  (2.5 mL), 80 °C, 12 h,  $\text{N}_2$  atmosphere; (vii)

Hydroalkylation product (0.2 mmol),  $\text{LiAlH}_4$  (0.1 mmol), THF (2 mL), 0 °C, 4 h,  $\text{N}_2$  atmosphere. **c** the MTT assays of **72**, **73** and ospemifene against MCF-7 cells; **(d)** the MTT assays of **72**, **73** and ospemifene against MDA-MB-231 cells; **(e)** mouse liver microsomal metabolic assays of **72** and ospemifene; **f** the MTT assays of **72** and ospemifene against MDA-10A. Experiments details were shown in the Supplementary Notes 3.3 Synthetic Applications. Data are presented as mean values  $\pm$  SD ( $n = 3$ ) biologically independent samples for panels **(c, d, f)**.

this alkene difunctionalization strategy, it opens a new window for organogermanes synthesis and is expected to stimulate substantial applications to functional materials and drug discovery.

## Methods

### General procedure for Ni-catalyzed gernylative alkylation of activated olefins

The procedure was conducted in a nitrogen-filled glove box. In an oven-dried 8 mL reaction vial equipped with a magnetic stir bar, alkene (0.45 mmol, 1.5 equiv.), germanium reagent (0.45 mmol, 1.5 equiv.),  $\text{NiBr}_2$  (10 mol%), Mn (0.9 mmol, 3.0 equiv.) and DMA (3 mL, 0.1 M) were charged and pre-stirred at 35 °C for 0.5 h, then alkyl

bromine (0.3 mmol, 1.0 equiv.) was added under  $\text{N}_2$ . The reaction vial was sealed and removed from the glove box. the mixture was stirred at 35 °C for another 36 h, subsequently quenched with water (10.0 mL) and extracted with dichloromethane ( $3 \times 15.0$  mL). The combined organic layers were washed with water, brine, dried over anhydrous  $\text{Na}_2\text{SO}_4$ , and concentrated under reduced pressure. The residue was purified by flash chromatography on silica gel to afford product.

### Reporting summary

Further information on research design is available in the Nature Portfolio Reporting Summary linked to this article.

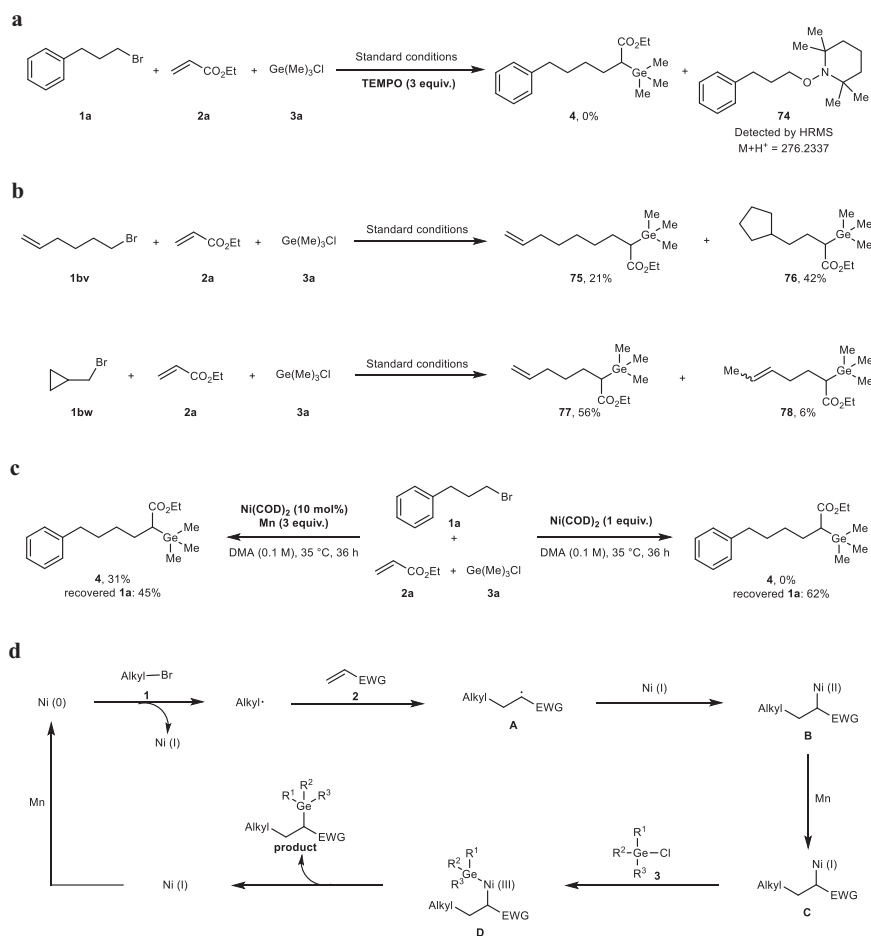


**Fig. 6 | Mechanism studies. a** radical trapping experiment. **b** radical-clock experiments. **c** control experiments. **d** proposed mechanism. Reaction details were

shown in the supplementary notes 3.4 Mechanistic Studies. TEMPO 2,2,6,6-tetramethyl-1-piperidinoxyl, COD 1,5-cyclooctadiene, EWG electron-withdrawing group.

## Data availability

The authors declare that the data supporting the findings of this study, including experimental details and compound characterization, are available within the article and its Supplementary Information file or source data file. Source data are provided with this paper. All other data are available from the corresponding author upon request.

## References

- Lan, X.-W., Wang, N.-X. & Xing, Y. Recent advances in radical difunctionalization of simple alkenes. *Eur. J. Org. Chem.* **2017**, 5821–5851 (2017).
- Wu, X., Wu, S. & Zhu, C. Radical-mediated difunctionalization of unactivated alkenes through distal migration of functional groups. *Tetrahedron. Lett.* **59**, 1328–1336 (2018).
- Zard, S. Z. The xanthate route to ketones: when the radical is better than the enolate. *Acc. Chem. Res.* **51**, 1722–1733 (2018).
- Bao, X. Z., Li, J., Jiang, W. & Huo, C. D. Radical-mediated difunctionalization of styrenes. *Synthesis* **51**, 4507–4530 (2019).
- Wu, Y.-C., Xiao, Y.-T., Yang, Y.-Z., Song, R.-J. & Li, J.-H. Recent advances in silver-mediated radical difunctionalization of alkenes. *Chem. Cat. Chem.* **12**, 5312–5329 (2020).
- Yu, X.-Y., Zhao, Q.-Q., Chen, J., Xiao, W.-J. & Chen, J.-R. When light meets nitrogen centered radicals: from reagents to catalysts. *Acc. Chem. Res.* **53**, 1066–1083 (2020).
- Siu, J. C., Fu, N. K. & Lin, S. Catalyzing electrosynthesis: a homogeneous electrocatalytic approach to reaction discovery. *Acc. Chem. Res.* **53**, 547–560 (2020).
- Jiang, H. & Studer, A. Intermolecular radical carboamination of alkenes. *Chem. Soc. Rev.* **49**, 1790–1811 (2020).
- Yao, H., Hu, W. & Zhang, W. Difunctionalization of alkenes and alkynes via intermolecular radical and nucleophilic additions. *Molecules* **26**, 105 (2021).
- Huang, H.-M., Bellotti, P., Ma, J., Dalton, T. & Glorius, F. Bifunctional reagents in organic synthesis. *Nat. Rev. Chem.* **5**, 301–321 (2021).
- Majhi, J. et al. Metal-free photochemical imino-alkylation of alkenes with bifunctional oxime esters. *J. Am. Chem. Soc.* **144**, 15871–15878 (2022).
- Tan, G. et al. Photochemical single-step synthesis of  $\beta$ -amino acid derivatives from alkenes and (Hetero)arenes. *Nat. Chem.* **14**, 1174–1184 (2022).
- Coombs, J. R. & Morken, J. P. Catalytic enantioselective functionalization of unactivated terminal alkenes. *Angew. Chem. Int. Ed.* **55**, 2636–2649 (2016).
- Yin, G., Mu, X. & Liu, G. Palladium(II)-catalyzed oxidative difunctionalization of alkenes: bond forming at a high-valent palladium center. *Acc. Chem. Res.* **49**, 2413–2423 (2016).
- Dong, Z., Ren, Z., Thompson, S. J., Xu, Y. & Dong, G. Transition-metal-catalyzed C–H alkylation using alkenes. *Chem. Rev.* **117**, 9333–9403 (2017).
- Zhang, J. S., Liu, L., Chen, T. & Han, L. B. Transition-metal-catalyzed three-component difunctionalizations of alkenes. *Chem. Asian J.* **13**, 2277–2291 (2018).
- Wang, Z.-X., Bai, X.-Y. & Li, B.-J. Metal-catalyzed substrate-directed enantioselective functionalization of unactivated alkenes. *Chin. J. Chem.* **37**, 1174–1180 (2019).



18. Li, Z.-L., Fang, G.-C., Gu, Q.-S. & Liu, X.-Y. Recent advances in copper-catalysed radical involved asymmetric 1,2-difunctionalization of alkenes. *Chem. Soc. Rev.* **49**, 32–48 (2020).
19. Feng, S., Dong, Y. & Buchwald, S. L. Enantioselective hydrocarbamoylation of alkenes. *Angew. Chem. Int. Ed.* **61**, e202206692 (2022).
20. Trammel, G. L. et al. Arylboration of enecarbamates for the synthesis of borylated saturated *N*-heterocycles. *Angew. Chem. Int. Ed.* **61**, e202212117 (2022).
21. Derosa, J., Apolinar, O., Kang, T., Tran, V. T. & Engle, K. M. Recent developments in nickel-catalyzed intermolecular dicarbofunctionalization of alkenes. *Chem. Sci.* **11**, 4287–4296 (2020).
22. Qi, X. & Diao, T. Nickel-catalyzed dicarbofunctionalization of alkenes. *ACS Catal.* **10**, 8542–8556 (2020).
23. Zhu, S., Zhao, X., Li, H. & Chu, L. Catalytic three-component dicarbofunctionalization reactions involving radical capture by nickel. *Chem. Soc. Rev.* **50**, 10836–10856 (2021).
24. Li, Y., Wu, D., Chen, H. G. & Yin, G. Difunctionalization of alkenes involving metal migration. *Angew. Chem. Int. Ed.* **59**, 7990–8003 (2020).
25. Pal, P. P., Ghosh, S. & Hajra, A. Recent advances in carbosilylation of alkenes and alkynes. *Org. Biomol. Chem.* **21**, 2272–2294 (2023).
26. Koike, T. & Akita, M. New horizons of photocatalytic fluoromethylative difunctionalization of alkenes. *Chem* **4**, 409–437 (2018).
27. Luo, Y., Tian, T., Nishihara, Y., Lv, L. & Li, Z. Iron-catalysed radical cyclization to synthesize germanium-substituted Indolo[2,1-*a*]isoquinolin-6(5*H*)-ones and Indolin-2-ones. *Chem. Commun.* **57**, 9276–9279 (2021).
28. Luo, Y., Xu, B., Lv, L. & Li, Z. Copper-catalyzed three-component germyl peroxidation of alkenes. *Org. Lett.* **24**, 2425–2430 (2022).
29. Luo, Y., Lv, L. & Li, Z. Copper-catalyzed germyl-azidation of alkenes with germanium hydrides and trimethylsilyl azide. *Org. Lett.* **24**, 8052–8056 (2022).
30. Tacke, R. et al. Syntheses and pharmacological characterization of achiral and chiral enantiopure C/Si/Ge-analogous derivatives of the muscarinic antagonist cycrimine: a study on C/Si/Ge bioisosterism. *J. Organomet. Chem.* **640**, 140–165 (2001).
31. Fujii, S., Miyajima, Y., Masuno, H. & Kagechika, H. Increased hydrophobicity and estrogenic activity of simple phenols with silicon and germanium-containing substituents. *J. Med. Chem.* **56**, 160–166 (2013).
32. Allard, N. et al. Germafluorenes: new heterocycles for plastic electronics. *Macromolecules* **43**, 2328–2333 (2010).
33. Kachian, J. S., Wong, K. T. & Bent, S. F. Periodic trends in organic functionalization of group IV semiconductor surfaces. *Acc. Chem. Res.* **43**, 346–355 (2010).
34. Su, T. A. et al. Silane and germane molecular electronics. *Acc. Chem. Res.* **50**, 1088–1095 (2017).
35. Fricke, C. & Schoenebeck, F. Organogermenes as orthogonal coupling partners in synthesis and catalysis. *Acc. Chem. Res.* **53**, 2715–2725 (2020).
36. Fricke, C. et al. Orthogonal nanoparticle catalysis with organogermenes. *Angew. Chem. Int. Ed.* **58**, 17788–17795 (2019).
37. Xu, M.-Y. et al. Alkyl carbagermatranes enable practical palladium-catalyzed sp<sup>2</sup>–sp<sup>3</sup> cross-coupling. *J. Am. Chem. Soc.* **141**, 7582–7588 (2019).
38. Sherborne, G. J. et al. Modular and selective arylation of aryl germanes (C–GeEt<sub>3</sub>) over C–Bpin, C–SiR<sub>3</sub> and halogens enabled by light-activated gold catalysis. *Angew. Chem. Int. Ed.* **59**, 15543–15548 (2020).
39. Dahiya, A., Fricke, C. & Schoenebeck, F. Gold-catalyzed chemoselective couplings of polyfluoroarenes with aryl germanes and downstream diversification. *J. Am. Chem. Soc.* **142**, 7754–7759 (2020).
40. Xi, Y. et al. Application of trimethylgermyl-substituted bisphosphine ligands with enhanced dispersion interactions to copper-catalyzed hydroboration of disubstituted alkenes. *J. Am. Chem. Soc.* **142**, 18213–18222 (2020).
41. Keil, P. M., Szilvási, T. & Hadlington, T. J. Reversible metathesis of ammonia in an acyclic germylene–Ni<sup>0</sup> complex. *Chem. Sci.* **12**, 5582–5590 (2021).
42. Xu, Q.-H., Wei, L.-P. & Xiao, B. Alkyl–GeMe<sub>3</sub>: neutral metalloid radical precursors upon visible-light photocatalysis. *Angew. Chem. Int. Ed.* **61**, e202115592 (2022).
43. Ura, Y., Hara, R. & Takahashi, T. Preparation of ethylene-bridged Group 14 metal–zirconocene complexes. *J. Organomet. Chem.* **611**, 299–303 (2000).
44. Nanjo, M., Oda, T. & Mochida, K. Preparation and structural characterization of trimethylsilyl-substituted germylzinc halides, (Me<sub>3</sub>Si)<sub>3</sub>GeZnX (X = Cl, Br, and I) and silylzinc chloride, R(Me<sub>3</sub>Si)<sub>2</sub>SiZnCl (R = SiMe<sub>3</sub> and Ph). *J. Organomet. Chem.* **672**, 100–108 (2003).
45. Kitching, W., Olszowy, H., Waugh, J. & Doddrell, D. Stereochemical aspects of substitution reactions of stannyl and germyl anionoids with cyclohexyl derivatives. *J. Org. Chem.* **43**, 898–906 (1978).
46. Kitching, W., Olszowy, H. A. & Harvey, K. Further studies of substitution reactions of stannyl and germyl anionoids with alkyl bromides. Rearrangement of the 6-hepten-2-yl moiety. *J. Org. Chem.* **47**, 1893–1904 (1982).
47. Xue, W., Mao, W., Zhang, L. & Oestreich, M. Mechanistic dichotomy of magnesium- and zinc-based germanium nucleophiles in the C(sp<sup>3</sup>)–Ge cross-coupling with alkyl electrophiles. *Angew. Chem. Int. Ed.* **58**, 6440–6443 (2019).
48. Lesbani, A. et al. Integrated palladium-catalyzed arylation of heavier group 14 hydrides. *Chem. Eur. J.* **16**, 13519–13527 (2010).
49. Komami, N., Matsuoka, K., Yoshino, T. & Matsunaga, S. Palladium-catalyzed germylation of aryl bromides and aryl triflates using hexamethyldigermene. *Synthesis* **50**, 2067–2075 (2018).
50. Selmani, A., Gevondian, A. G. & Schoenebeck, F. Germylation of arenes via Pd(I) dimer enabled sulfonium salt functionalization. *Org. Lett.* **22**, 4802–4805 (2020).
51. Su, P.-F. et al. Nickel-catalyzed reductive C–Ge coupling of aryl/alkenyl electrophiles with chlorogermenes. *Angew. Chem. Int. Ed.* **60**, 26571–26576 (2021).
52. Guo, P. et al. Nickel-catalyzed reductive Csp<sup>3</sup>–Ge coupling of alkyl bromides with chlorogermenes. *Org. Lett.* **24**, 1802–1806 (2022).
53. Kanyiva, K. S., Kuninobu, Y. & Kanai, M. Palladium-catalyzed direct C–H silylation and germanylation of benzamides and carboxamides. *Org. Lett.* **16**, 1968–1971 (2014).
54. Murai, M., Takeshima, H., Morita, H., Kuninobu, Y. & Takai, K. Acceleration effects of phosphine ligands on the rhodium-catalyzed dehydrogenative silylation and germylation of unactivated C(sp<sup>3</sup>)–H bonds. *J. Org. Chem.* **80**, 5407–5414 (2015).
55. Deb, A. et al. Experimental and computational studies on remote γ-C(sp<sup>3</sup>)–H silylation and germanylation of aliphatic carboxamides. *ACS Catal.* **7**, 8171–8175 (2017).
56. Zhou, Z.-X., Rao, W.-H., Zeng, M.-H. & Liu, Y.-J. Facile synthesis of unnatural β-germyl-α-amino amides via Pd(II)-catalyzed primary and secondary C(sp<sup>3</sup>)–H bond germylation. *Chem. Commun.* **54**, 14136–14139 (2018).
57. Fischer, A. K., West, R. C. & Rochow, E. G. The addition reaction between trichlorogermane and an olefin. *J. Am. Chem. Soc.* **76**, 5878 (1954).
58. Wolfsberger, W. Hydrogermylierungsreaktionen. *J. Prakt. Chem./Chem.-Ztg.* **334**, 453–464 (1992).
59. Trofimov, A., Rubina, M., Rubin, M. & Gevorgyan, V. Highly diastereo- and regioselective transition metal-catalyzed additions of metal hydrides and bimetallic species to cyclopropenes: easy

- access to multisubstituted cyclopropanes. *J. Org. Chem.* **72**, 8910–8920 (2007).
60. Ahrens, T., Telteuws, M., Ahrens, M., Braun, T. & Laubenstein, R. Competing reaction pathways of 3,3,3-trifluoropropene at rhodium hydrido, silyl and germyl complexes: C–F bond activation versus hydrogermylation. *Dalton Trans.* **45**, 17495–17507 (2016).
61. Wollenburg, M. et al. Palladium-catalyzed disilylation and digermanylation of alkene tethered aryl halides: direct access to versatile silylated and germanylated heterocycles. *Org. Lett.* **22**, 3679–3683 (2020).
62. Lin, W., You, L., Yuan, W. & He, C. Cu-catalyzed enantioselective hydrogermylation: asymmetric synthesis of unnatural  $\beta$ -germyl  $\alpha$ -amino acids. *ACS Catal.* **12**, 14592–14600 (2022).
63. Keess, S. & Oestreich, M. Access to fully alkylated germanes by  $B(C_6F_5)_3$ -catalyzed transfer hydrogermylation of alkenes. *Org. Lett.* **19**, 1898–1901 (2017).
64. Xu, N.-X., Li, B.-X., Wang, C. & Uchiyama, M. Sila- and germa-carboxylic acids: precursors for the corresponding silyl and germyl radicals. *Angew. Chem. Int. Ed.* **59**, 10639–10644 (2020).
65. Queen, A. E., Selmani, A. & Schoenebeck, F. Hydrogermylation of alkenes via organophotoredox-initiated HAT catalysis. *Org. Lett.* **24**, 406–409 (2022).
66. Ritchie, T. J. & Macdonald, S. J. F. The impact of aromatic ring count on compound developability - are too many aromatic rings a liability in drug design? *Drug Discov. Today* **14**, 1011–1020 (2009).
67. Lovering, F. Escape from flatland 2: complexity and promiscuity. *Med. Chem. Comm.* **4**, 515–519 (2013).
68. Caplin, M. J. & Foley, D. J. Emergent synthetic methods for the modular advancement of  $sp^3$ -rich fragments. *Chem. Sci.* **12**, 4646–4660 (2021).
69. Taras, T. L., Wurz, G. T. & DeGregorio, M. W. In vitro and in vivo biologic effects of ospemifene (FC-1271a) in breast cancer. *J. Steroid Biochem. Mol. Biol.* **77**, 271–279 (2001).
70. Kaur, G. et al. Design, synthesis and evaluation of ospemifene analogs as anti-breast cancer agents. *Eur. J. Med. Chem.* **86**, 211–218 (2014).

## Acknowledgements

We gratefully acknowledge the financial support of the “Thousand Talents Plan” Youth Program (X.Z.), the “Jiangsu Specially-Appointed Professor Plan” (R2020T30, X.Z.), the “Innovation & Entrepreneurship Talents Plan” (X.Z.), the National Natural Science Foundations of China (22101136, X.Z. and 22172014, M.B.), LiaoNing Revitalization Talents Program (XLYC1802030, M.B.) and the Natural Science Foundation of Jiangsu Province (BK20200806, X.Z.). We also thank Prof. Guangzhe Li (Dalian University of Technology) for supplying breast cancer cells and

experimental instruments, Shanghai Medicilon company for the mouse liver microsomal metabolic assay and Prof. Andrew McNally (Colorado State University) for assistance with the manuscript proofing.

## Author contributions

X.Z. conceived the project. R.G. conducted experiments. X.Z. and M.B. supervised the research and wrote the manuscript with the assistance of other authors. All the authors analyzed the data.

## Competing interests

The authors declare no competing interests.

## Additional information

**Supplementary information** The online version contains supplementary material available at <https://doi.org/10.1038/s41467-023-43561-z>.

**Correspondence** and requests for materials should be addressed to Ming Bao or Xuan Zhang.

**Peer review information** *Nature Communications* thanks Damiano Tanini and the other, anonymous, reviewer(s) for their contribution to the peer review of this work. A peer review file is available.

**Reprints and permissions information** is available at <http://www.nature.com/reprints>

**Publisher’s note** Springer Nature remains neutral with regard to jurisdictional claims in published maps and institutional affiliations.

**Open Access** This article is licensed under a Creative Commons Attribution 4.0 International License, which permits use, sharing, adaptation, distribution and reproduction in any medium or format, as long as you give appropriate credit to the original author(s) and the source, provide a link to the Creative Commons licence, and indicate if changes were made. The images or other third party material in this article are included in the article’s Creative Commons licence, unless indicated otherwise in a credit line to the material. If material is not included in the article’s Creative Commons licence and your intended use is not permitted by statutory regulation or exceeds the permitted use, you will need to obtain permission directly from the copyright holder. To view a copy of this licence, visit <http://creativecommons.org/licenses/by/4.0/>.

© The Author(s) 2023